A Blob Model To Study Chain Folding by Fluorescence

Anna K. Mathew, Howard Siu, and Jean Duhamel*

Institute for Polymer Research, Department of Chemistry, University of Waterloo, Waterloo, ON N2J 3G1, Canada

Received May 4, 1999; Revised Manuscript Received August 16, 1999

ABSTRACT: Monodisperse polystyrenes ($M_w/M_n < 1.15$) with molecular weights of 6K, 40K, and 110K and one polydisperse polystyrene ($M_w/M_n = 1.5$) with a molecular weight of 110K were synthesized. The chromophore pyrene was randomly and covalently attached onto the polymers. The dynamics of the chains were investigated quantitatively by monitoring the fluorescence of the pyrene monomer. The polymer coil was divided into several blobs among which pyrene is randomly distributed according to a Poisson distribution. The kinetics of the pyrene groups are monitored by only three parameters: k_{diff}, the rate at which one excited pyrene encounters one ground state (GS) pyrene inside a blob; k_e[blob], the product characterizing the exchange of GS pyrene between blobs (k_e is the rate of exchange and [blob] is the blob concentration inside the polymer coil); and $\langle n \rangle$, the average number of GS pyrene per blob. We show that the parameters retrieved by this analysis are internally consistent within the theoretical framework of the blob model. A critical polymer chain length is found above which polymer chain dynamics behave in a similar manner, regardless of the size of the polymer. Below the critical polymer chain length, chain dynamics are chain length-dependent.

Introduction

Fluorescence dynamic quenching (FDQ) is a powerful technique for monitoring polymer chain dynamics in solution.[1] In a FDQ experiment, a dye is covalently attached onto a polymer chain with an appropriate quencher. In this report, we used FDQ to monitor the chain-folding mechanism of model polymer chains. The pyrene chromophore was randomly and covalently attached onto a polystyrene backbone. Pyrene is often chosen to monitor polymer properties by fluorescence.[1,2] Upon absorption of a photon, pyrene becomes excited and can either fluoresce in the blue region (∼380 nm) or encounter a ground state (GS) pyrene by diffusion and form a complex called an excimer.[3] The excimer fluoresces in the green region (∼480 nm). Excimer formation results in the quenching of the pyrene monomer fluorescence so that the same molecule plays the part of both the dye and its quencher. At low concentration where only intramolecular excimer formation occurs, the extent of excimer formation yields information about the polymer flexibility; i.e., a stiff polymer forms only a limited amount of excimer. Fluorescence lifetime measurements yield information about the rates at which the excimer is formed. Because the pyrene groups are covalently attached onto the polymer, excimer formation indicates that two polymer segments have come in contact. Thus, excimer formation rates yield information about the dynamics of the chain-folding process.

To date, quantitative kinetic information about the process of excimer formation between pyrenes attached on a polymer chain can be retrieved *only* if the pyrene groups are attached at two specific positions on the chain, usually at the chain ends.[2] The kinetics of excimer formation are depicted in Scheme 1, which is a version of Birks' Scheme[3] applied to polymer systems. τ_M and τ_E are the lifetimes of the monomer and excimer, respectively. k_{-1} is the dissociation rate of the excimer. The rate of excimer formation $\langle k_1 \rangle$ is a pseudo-unimolecular rate constant. The local pyrene concentration $[Py]_{loc}$ within the polymer coil is difficult to estimate and

Scheme 1. Birks' Scheme for Pyrene End-Labeled Polymer Chains

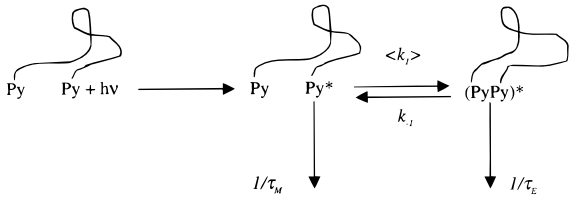

one uses $\langle k_1 \rangle$ to represent the product $k_1[Py]_{loc}$, where k_1 is the bimolecular rate constant of excimer formation. When pyrene groups are attached at the ends of monodisperse polymers of different lengths, the rate constants $\langle k_1 \rangle$, which are retrieved from the analysis of the fluorescence decays, show a strong dependence with polymer chain length.[2]

This chain length dependence makes it rather difficult to analyze quantitatively by fluorescence the behavior of a polymer coil randomly labeled with pyrene. A priori, one would expect the interior of the randomly labeled polymer coil to be a microvolume where pyrene behaves in the same manner as in a homogeneous solution. This simple and idealistic picture is, unfortunately, inappropriate. Random labeling of pyrene groups along the polymer backbone induces a distribution of chain lengths between any two chromophores on the chain, which results in a distribution of excimer formation rate constants.[4] This distribution makes more difficult the analysis of the fluorescence decays, which are typically described as *complicated*. Qualitative information is obtained by calculating the average lifetime of the fluorescence decays.[5]

Although quantitative information about chain dynamics can be retrieved by fluorescence spectroscopy when the pyrene groups are attached at two specific positions of the polymer chains, the only dynamic information retrieved from these measurements is the rate at which these two specific segments encounter each other. A much more global picture of the chain-folding mechanism would be obtained by monitoring the

10.1021/ma990702c CCC: $18.00
Published on Web 10/01/1999

behavior of polymer chains displaying pyrene groups randomly attached along the backbone. The purpose of this work is to demonstrate that it is possible to obtain quantitative information about the folding mechanism of polymer chains by monitoring the fluorescence decays of polymer chains randomly labeled with the chromophore pyrene.

Theory

Scheme 2 represents a chain that has been randomly labeled with pyrene. It is clear from Scheme 2 that the pyrene concentration fluctuates within the polymer coil and that domains form in the three-dimensional representation of the polymer coil. In Scheme 2, Py**2**, Py**3**, Py**4**, and Py**5** form a pyrene-rich domain, whereas Py**1**, Py**6**, and Py**7** are rather isolated.

To handle this situation mathematically, the polymer coil was divided into blobs (cf. Scheme 3A). The pyrene groups distribute themselves randomly into the blobs according to a Poisson probability.[6,7]

If the dissociation rate k_{-1} for the pyrene excimer is assumed to equal 0 s^{-1} (k_{-1} is usually small for pyrene[3]), the process of excimer formation can be described by eqs 1−4. The blobs are defined as a volume larger than or equal to that probed by an excited pyrene during its lifetime. A consequence of this definition of a blob is that an excited pyrene cannot leave a blob while remaining in the excited state. On the other hand, GS pyrenes, which have an infinite lifetime, can diffuse in and out of the blobs.

process = fluorescence

$$\mathrm{Py}^*_{\mathrm{diff},n} \rightarrow \mathrm{Py}_{\mathrm{diff},n} \quad (1)$$

$$\text{rate} = 1/\tau_{\mathrm{M}}$$

process = exchange

$$\mathrm{Py}^*_{\mathrm{diff},n} + \mathrm{Py}_{\mathrm{diff},j} \rightarrow \mathrm{Py}^*_{\mathrm{diff},\,n+1} + \mathrm{Py}_{\mathrm{diff},\,j-1} \quad (2)$$

$$\text{rate} = jk_{\mathrm{e}}\mathrm{Py}^*_{\mathrm{diff},n}\mathrm{Py}_{\mathrm{diff},\,j}$$

process = exchange

$$\mathrm{Py}^*_{\mathrm{diff},n} + \mathrm{Py}_{\mathrm{diff},j} \rightarrow \mathrm{Py}^*_{\mathrm{diff},\,n-1} + \mathrm{Py}_{\mathrm{diff},\,j+1} \quad (3)$$

$$\text{rate} = nk_{\mathrm{e}}\mathrm{Py}^*_{\mathrm{diff},n}\mathrm{Py}_{\mathrm{diff},j}$$

process = excimer formation

$$\mathrm{Py}^*_{\mathrm{diff},n} \rightarrow E^* \quad (4)$$

$$\text{rate} = nk_{\mathrm{diff}}$$

In eqs 1−4, $\mathrm{Py}^*_{\mathrm{diff},\,n}$ is the number of blobs containing one excited pyrene and n GS pyrenes. $\mathrm{Py}^*_{\mathrm{diff},\,j}$ is the number of blobs containing j GS pyrenes. The rate constants k_{e} and k_{diff} are shown in Scheme 3B. k_{e} is the rate of exchange of GS pyrenes among blobs. k_{diff} is the diffusion-controlled rate of encounter inside a blob containing one excited pyrene and one GS pyrene. k_{diff} is a pseudo-unimolecular rate constant. It includes a concentration term ($[\mathrm{Py}]_{\mathrm{loc}}$) equivalent to one GS pyrene inside one blob ($[\mathrm{Py}]_{\mathrm{loc}} = N_{\mathrm{A}}/V_{\mathrm{blob}}$ where V_{blob} is the volume of a blob and N_{A} is Avogadro's number). These equations are adapted from those that were derived for micellar systems.[8,9,17] According to the classic mathematical derivation of Tachiya,[9a] one obtains eq 5 as the time-dependent concentration profile of free excited pyrene disappearing via excimer formation:

Scheme 2. Three-Dimensional Representation of a Polymer Chain[21] Randomly Labeled with Pyrene

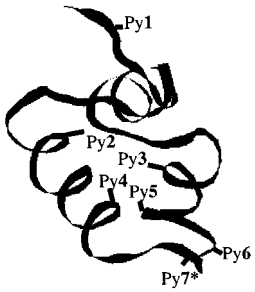

Scheme 3. Three-Dimensional Blob Representations of a Polymer Chain Randomly Labeled with Pyrene. (A) With the Polymer Chain in the Background. (B) Without the Polymer Chain[a]

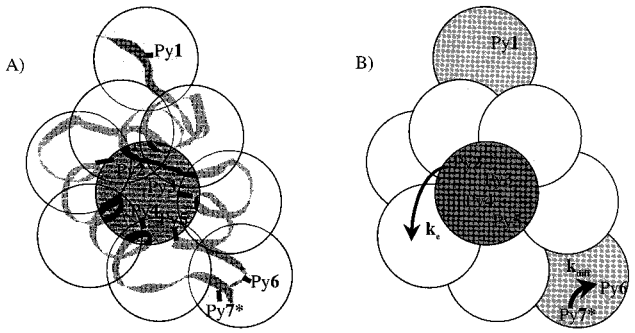

[a] The dark and light gray areas are pyrene-rich and -poor, respectively, and the white areas enclosed by circles are devoid of pyrene. The rate constants k_{e} and k_{diff} are shown in part B.

$$[\mathrm{Py}^*_{\mathrm{diff}}]_{(t)} = [\mathrm{Py}^*_{\mathrm{diff}}]_{(t=0)} \exp\{-(k_{\mathrm{f}} + A_2)t - A_3[1 - \exp(-A_4 t)]\} \quad (5)$$

where the constants A_i are the following:

$$A_2 = \langle n\rangle \frac{k_{\mathrm{diff}}k_{\mathrm{e}}[\mathrm{blob}]}{k_{\mathrm{diff}} + k_{\mathrm{e}}[\mathrm{blob}]} \quad A_3 = \langle n\rangle \frac{k_{\mathrm{diff}}^2}{(k_{\mathrm{diff}} + k_{\mathrm{e}}[\mathrm{blob}])^2} \quad A_4 = k_{\mathrm{diff}} + k_{\mathrm{e}}[\mathrm{blob}] \quad (6)$$

with [blob] being the local concentration of blobs inside the polymer coil and $\langle n\rangle$ being the average number of GS pyrenes inside the blobs. Equation 5 is very similar to that derived by Infelta et al.[9b] for micellar systems and can also be applied to the study of associating polymers.[10]

Polymer systems usually follow scaling laws, and a blob approach is often very convenient to describe them. Theories on polymer systems can involve theoretical blobs. A theoretical blob can be defined as the volume containing a given polymer mass having an energy $k_{\mathrm{B}}T$, where k_{B} is the Boltzmann constant and T is the absolute temperature expressed in Kelvin.[11] An analysis using the concept of a blob shifts the focus of the study from the entire polymer chain to a single blob. As a result, such an analysis can handle polydisperse systems. A long polymer chain will contain several blobs; a short one will contain only a few blobs. We will show that our blob analysis is robust and can also handle polydisperse polymeric systems.

The blob approach, which we are proposing to investigate polymer chain dynamics by fluorescence, relies on only three parameters: k_{diff}, $\langle n\rangle$, and the product

k_e[blob]. To the best of our knowledge, it is the simplest approach for analyzing fluorescence decays of pyrene randomly attached onto a polymer backbone. It is also fundamentally different from any other approach used in this area because it introduces a concept rarely used in the field of FDQ, the concept of a blob.

Experimental Section

Synthesis of Monodisperse Polystyrene. All of the monodisperse polymers used in the present study were prepared by anionic polymerization.[12] Tetrahydrofuran (THF, Caledon) was dried by refluxing with sodium benzophenone under inert nitrogen. The styrene monomer (Aldrich, 99%) was purified by two distillations over CaH_2 under reduced pressure. Styrene was further dried with phenylmagnesium chloride (Aldrich, 2.0 M in THF) and degassed by freeze−thaw cycles, followed by slow recondensation to an ampule. Polymerization of styrene was initiated by *sec*-butyllithium (Aldrich, 1.3 M in cyclohexane) in dry THF (20 mL of THF/g of styrene) under an inert atmosphere. After 30 min, the polymerization reaction was stopped by injecting 1 mL of degassed methanol into the reactor. The polystyrene solution was precipitated in methanol, filtered, and dried under vacuum. Monodisperse polymers of various molecular weights were prepared by changing the styrene monomer-to-initiator ratio.

Synthesis of Polydisperse Polystyrene. Polydisperse polystyrenes were prepared by free radical polymerization. Styrene monomer was washed three times with a 10% aqueous solution of NaOH to remove the inhibitor. It was again washed with water three times and passed through a bed of anhydrous sodium sulfate. The monomer was then distilled under reduced pressure. The polymerization was carried out using azobis(isobutyronitrile) (AIBN, Aldrich) as the initiator at a concentration of 3×10^{-3} mol/L of a 30% w/w styrene monomer solution in toluene at 60 °C for 24 h. The polymer was precipitated in methanol.

Chloromethylation of Polystyrene. The polystyrenes were chloromethylated by a Friedel−Crafts alkylation using chloromethyl methyl ether (CMME).[13] CMME is a known carcinogen, and any reaction involving the use of CMME was carried out in a well-ventilated fume hood. Aluminum chloride was used as the catalyst, and 1-nitropropane was utilized as a modifier to reduce the activity of $AlCl_3$ and to control potential cross-linking of the polystyrene. CMME was prepared from decanoyl chloride and dimethoxymethane.[14] A 1% catalyst solution was prepared by dissolving aluminum chloride in a 1:3 carbon tetrachloride/nitropropane mixture. Polystyrene (0.3 g) was dissolved in 50 mL of dry carbon tetrachloride and was kept under stirring. CMME (3 mL) was added, followed by 6 mL of the catalyst solution. The reaction was allowed to proceed for 30 min and was terminated with 0.5 mL of glacial acetic acid. The solvent and CMME were removed under vacuum, and the polymer was redissolved in a minimum amount of chloroform. The catalyst was extracted with a 1:1 mixture of acetic acid and water, and the polymer was precipitated in methanol. The chloromethylation level was determined by ^{1}H NMR spectroscopy. Varying the amount of catalyst solution varied the chloromethylation level.

Pyrene Labeling. The chloromethylated polystyrene (0.25 g) and 1-pyrenemethanol (5 equiv, on the basis of the chloromethylation level) were introduced into an ampule that was then evacuated and put under nitrogen environment. Dry and freshly distilled DMF (40 mL) was added, followed by sodium hydride (10 equiv, on the basis of chloromethylation level). The ampule was placed in a 60 °C oil bath under stirring, and the reaction was allowed to proceed for 72 h. The DMF was partially removed under vacuum. The polymer was precipitated from DMF by water. The resulting polymer was purified by repeated precipitation from tetrahydrofuran by methanol until the polymer is completely freed of unreacted pyrenemethanol.

Absorption Measurements. A Hewlett-Packard 8452A diode array spectrophotometer was used for the absorption measurements.

Pyrene Content of Polymer Samples. The pyrene content of the polymer was established by measuring the absorption of a solution prepared from a carefully weighed amount (m) of pyrene-labeled polymer in a known volume of THF (V). The pyrene concentration [Py] was then estimated from the absorption value at 344 nm and the extinction coefficient of a pyrene model compound, typically 1-pyrenemethanol (ϵ [344 nm, in THF] = 42 700 $cm^{-1}M^{-1}$, measured in the laboratory). The pyrene content, λ, of the polymer could be calculated from $\lambda = [Py]V/m$ expressed in moles of pyrene per gram of polymer.

Steady-State Fluorescence Spectroscopy. Steady-state fluorescence spectra were recorded on a Photon Technology International LS-100 steady-state system with a pulsed xenon flash lamp as the light source. The slit widths on the excitation and emission monochromators equaled 2 and 1 nm, respectively. All spectra were obtained with the usual right-angle configuration. The polymer solutions were degassed under a gentle flow of nitrogen and had a pyrene concentration of 2.5×10^{-6} M in THF (distilled in glass, Caledon) to avoid intermolecular excimer formation. The samples were excited at 344 nm. The spectra were normalized at 375 nm. The fluorescence intensities of the monomer (I_M) and of the excimer (I_E) were calculated by taking the integrals under the fluorescence spectra from 372 to 378 nm for the pyrene monomer, and from 500 to 530 nm for the pyrene excimer. The excimer fluorescence intensity is considered for wavelengths above 500 nm to avoid potential overlap with the pyrene monomer fluorescence.

Time-Resolved Fluorescence Spectroscopy. Decay curves were obtained by the time-correlated single-photon counting technique. These were measured by a Photochemical Research Associates, Inc., System 2000. The excitation wavelength was 344 nm, and the fluorescence from the pyrene monomer and excimer was monitored at 375 and 510 nm, respectively. To block potential light scattering leaking through the detection system, filters were used with cutoffs at 370 and 495 nm to acquire the fluorescence decays of the pyrene monomer and excimer, respectively. All decays were collected over 512 channels. A total of 20 000 counts was collected at the peak maximum of the lamp and the decay curves. The analyses of the decay curves were performed with the δ-pulse deconvolution.[15] Reference decay curves of degassed solutions of PPO [2,5-diphenyloxazole] in cyclohexane (τ = 1.42 ns)[16a] and BBOT [2,5-bis(5-*tert*-butyl-2-benzoxazolyl)thiophene] in ethanol (τ = 1.47 ns)[16b] were used for the analyses of the monomer and excimer decay curves, respectively. The polymer solutions were degassed under a gentle flow of nitrogen and the pyrene concentration was kept at 2.5×10^{-6}M in THF (distilled in glass, Caledon) to avoid intermolecular excimer formation.

Analysis of the Fluorescence Decays. Fluorescence decays of the pyrene excimer were recorded. Solutions were excited at 344 nm, and the fluorescence was collected at 510 nm. The decays were fitted with a sum of three exponentials according to eq 7.

$$i_E(t) = a_{E1} \exp(-t/\tau_{E1}) + a_{E2} \exp(-t/\tau_{E2}) + a_{E3} \exp(-t/\tau_{E3}) \quad (7)$$

All decays exhibited a rise time, and a_{E1} was negative. The ratio $a_{E1}/(a_{E2} + a_{E3})$ was always more positive than −1.0, indicating that some pyrene groups were preassociated. This is reasonable because the labeling occurs randomly and two neighboring styrene units can harbor a pyrene group. The close vicinity of such pyrene groups induces excimer formation on a subnanosecond time scale, which is too short to be properly probed by our time-resolved spectrofluorometer but introduces some slight distortions at the early times of our fluorescence decays. This fast excimer formation process was accounted for by introducing a correction usually referred to as light scat-

tering correction in the analysis of the monomer fluorescence decays.[15] The monomer fluorescence decays were fitted by either a triexponential given in eq 8 or by the more complicated eq 11, which is commonly used to deal with micellar systems.[8,9,17]

$$i_M(t) = a_{M1}\exp(-t/\tau_{M1}) + a_{M2}\exp(-t/\tau_{M2}) + a_{M3}\exp(-t/\tau_{M3}) \quad (8)$$

$i_M(t)$ was convoluted with the instrument response function $L(t)$. The light scattering correction was implemented by adding the instrument response function to the convolution product according to eq 9:

$$I_M(t) = i_M(t) \otimes L(t) + a_{scatt}L(t) \quad (9)$$

where the symbol $\otimes$ indicates the convolution and a_{scatt} indicates the fraction of light scattering correction being applied. The resulting function $I_M(t)$ was then compared with the experimental fluorescence decay, and the parameters of either eq 8 or 11 were optimized using the Marquardt−Levenberg algorithm.[18]

Gel Permeation Chromatography. The samples were analyzed with a Waters SEC system using THF as an eluent and a Jordi linear DVB mixed-bed column. The instrument was coupled with a DRI detector. The column was calibrated using known molecular weight polystyrene standards. These experiments were carried out at room temperature.

Results

The chain dynamics of four polystyrenes were studied in THF by fluorescence spectroscopy. 6K, 40K, and 110K polystyrenes were synthesized by anionic polymerization. They were monodisperse ($M_w/M_n < 1.15$) and are referred to as MD6K, MD40K, and MD110K, respectively. The fourth polymer was synthesized by radical polymerization. It had a molecular weight of 110K and a polydispersity M_w/M_n of 1.5. It is referred to as PD110K. Each polystyrene sample was then labeled with pyrene. Polystyrene was chloromethylated, followed by the nucleophilic substitution of the chloride of the chloromethyl groups by pyrenemethoxide formed by the reaction of pyrenemethanol with sodium hydride. The pyrene content of the polymer was described by either the percentage of styrene monomers carrying a pyrene group (expressed in mole percent) or the number of moles of pyrene per gram of polymer (λ). A minimum of four different pyrene contents ranging from 1 to 12 mol % was obtained for each polymer sample. The polymer chain-length distributions and polydispersity indexes were characterized by gel permeation chromatography. The M_n, M_w/M_n, and pyrene content of each sample are listed in Table 1. The molecular weights and polydispersities were found to remain the same within experimental error after the chloromethylation and pyrene labeling reaction.

For a given polymer sample, steady-state fluorescence spectra were recorded. The polymer concentrations were kept low in order to prevent intermolecular excimer formation. The pyrene concentration determined by absorption measurements equaled 2.5×10^{-6} M. Figure 1 reports the spectra obtained for the MD110K polystyrene. They were normalized at 375 nm, which corresponds to the 0−0 peak. Figure 1 shows that as the pyrene content of the polymer increases more excimer is being formed intramolecularly, as expected. The fluorescence intensity of the pyrene monomer I_M was calculated by measuring the area under the fluorescence spectra from 372 to 378 nm. The fluorescence intensity of the excimer I_E was determined by measuring the area under the fluorescence spectra from 500 to 530 nm.

Table 1. Parameters Retrieved from the Triexponential Fit of the Pyrene Monomer Fluorescence Decays of Pyrene-Labeled Polystyrenes in THF

sample M_n; M_w/M_n	pyrene (mol %)	τ_{M1} (ns)	a_{M1}	τ_{M2} (ns)	a_{M2}	τ_{M3} (ns)	a_{M2}	χ^2
MD110K	1.08	33	0.31	138	0.55	257	0.14	1.09
113 000; 1.03	1.26	31	0.31	125	0.51	257	0.18	1.08
	2.40	26	0.5	91	0.39	257	0.10	1.14
	2.54	23	0.5	79	0.47	257	0.02	1.33
	4.59	18	0.67	59	0.33	257	0.01	1.41
	7.03	12	0.76	41	0.24	257	0.00	1.71
MD40K	1.65	31	0.36	121	0.47	257	0.17	0.98
40 000; 1.04	2.23	33	0.48	116	0.45	257	0.07	1.27
	4.86	18	0.65	65	0.33	257	0.01	1.37
	5.98	14	0.76	49	0.21	257	0.02	1.30
PD110K	1.30	30	0.36	116	0.52	257	0.10	1.04
110 000; 1.48	3.17	22	0.55	84	0.38	257	0.07	1.35
	6.15	15	0.71	53	0.26	257	0.03	1.56
	6.29	15	0.73	49	0.26	257	0.01	1.22
	6.86	13	0.74	44	0.25	257	0.01	1.36
MD6K	3.03	18	0.35	84	0.36	257	0.28	1.12
6000; 1.13	4.33	15	0.41	68	0.36	257	0.22	1.55
	8.86	15	0.66	64	0.24	257	0.10	1.22
	11.06	18	0.67	74	0.23	257	0.10	1.30

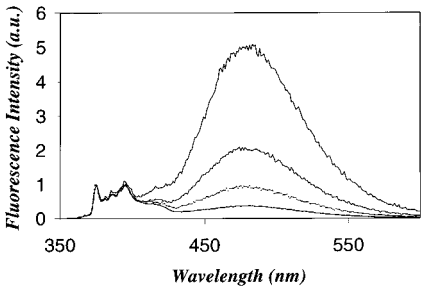

Figure 1. Fluorescence spectra of MD110K randomly labeled with pyrene. Pyrene content from bottom to top: 1.3, 2.5, 4.6, and 7.0 mol %. The pyrene concentration of these polymer solutions in THF equals 2.5×10^{-6} M.

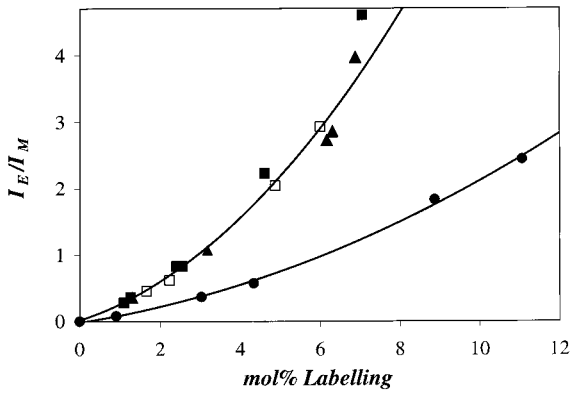

Figure 2. Ratio I_E/I_M as a function of pyrene content in mole percent. ● MD6K, □ MD40K, ■ MD110K, and ▲ PD110K. The pyrene concentration of these polymer solutions in THF equals 2.5×10^{-6} M.

Figure 2 reports the I_E/I_M ratios obtained for the four polymers. In the case of homogeneous pyrene solutions, the ratio I_E/I_M is directly proportional to the pyrene concentration.[3] For all polymer samples, I_E/I_M increases with pyrene content. A quadratic expression with no physical meaning was used to fit the I_E/I_M ratios in Figure 2 to help visualize the increase in the I_E/I_M ratio with the increase in pyrene content. This increase agrees qualitatively well with the expected behavior of

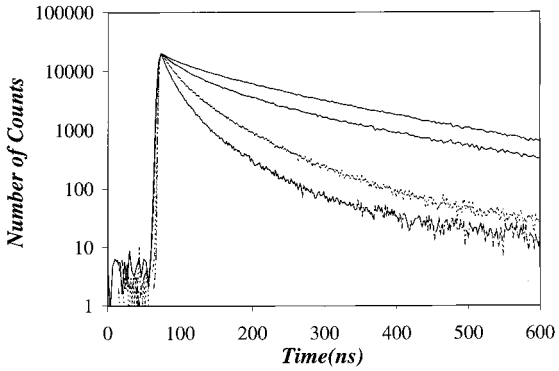

Figure 3. Fluorescence decays of the pyrene monomer (λ_{ex} = 344 nm, λ_{em} = 375 nm) for MD110K. Pyrene content from bottom to top: 1.3, 2.5, 4.6, and 7.0 mol %. The pyrene concentration of these polymer solutions in THF equals 2.5×10^{-6} M.

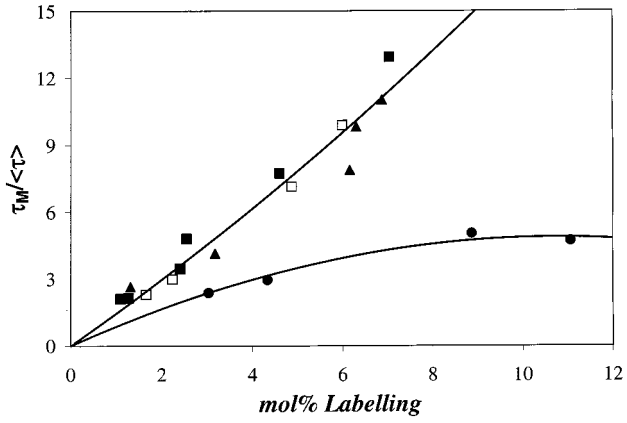

Figure 4. Ratio $\tau_M/\langle\tau\rangle$ as a function of pyrene content in mole percent. ● MD6K, □ MD40K, ■ MD110K, and ▲ PD110K. The pyrene concentration of these polymer solutions in THF equals 2.5×10^{-6} M.

the I_E/I_M ratio in homogeneous solutions. However, there is no linear correspondence between the I_E/I_M ratio and the pyrene content of the polymer. This indicates that the kinetics of excimer formation within a polymer coil do not mimic those describing pyrene excimer formation in homogeneous solutions. The I_E/I_M ratios fall on the same master curve for the MD40K, MD110K, and PD110K polymers. The I_E/I_M ratios for the shorter MD6K polymer lie clearly outside the master curve.

Fluorescence decay measurements of the pyrene monomer were carried out on all of the polymer samples. Solutions were excited at 344 nm, and the fluorescence was collected at 375 nm. Figure 3 represents the fluorescence decays obtained for the pyrene monomer of the MD110K sample. Higher pyrene content led to an increased fluorescence quenching of the monomer, and the time-resolved fluorescence spectra exhibit a faster decay. The monomer fluorescence decays were first fitted with three exponentials according to eq 9 where the function $i_M(t)$ is given by eq 8.

The third decay time, τ_{M3}, was fixed to equal τ_M, the pyrene monomer lifetime. τ_M was determined by fitting the fluorescence decays of pyrene-labeled polystyrene samples having pyrene content lower than 0.2%. With such a low labeling level, very few excimers are formed, and the long component of the decay represents the emission of unquenched excited pyrenes. The natural lifetime of pyrene attached onto polystyrene ($\tau_M = k_f^{-1}$) was found to equal 257 ns. Pyrenemethanol in THF has a lifetime of 245 ns. The fact that the lifetime of pyrene attached onto polystyrene is slightly longer than that of pyrenemethanol indicates that the polymer coil is protecting the chromophores, as it has been already reported in a few instances.[19] Because the lifetime increase is small, the coil protection has a limited effect.

The preexponential factors a_{Mi} and decay times τ_{Mi} (with $i = 1-3$) obtained by fitting the fluorescence decays with eq 9, using eq 8 for $i_M(t)$, are listed in Table 1. We note that the χ^2 are relatively high (eight χ^2 out of nineteen are above 1.3), which indicates that the fits are not perfect. The average decay times of the fluorescence decays were calculated with eq 10.

$$\langle\tau\rangle = \frac{a_{M1}\tau_{M1} + a_{M2}\tau_{M2} + a_{M3}\tau_{M3}}{a_{M1} + a_{M2} + a_{M3}} \qquad (10)$$

A plot of $\tau_M/\langle\tau\rangle$ versus pyrene content for the different polymers is given in Figure 4. When the pyrene content increases, more excimers are being formed and the average decay time of the pyrene monomer decreases. Consequently, the ratio $\tau_M/\langle\tau\rangle$ increases with pyrene content. The behavior exhibited by the ratio $\tau_M/\langle\tau\rangle$ in Figure 4 is very similar to that obtained for I_E/I_M in Figure 2. The three longer polymers MD40K, MD110K, and PD110K exhibit a similar trend for $\tau_M/\langle\tau\rangle$, which is clearly different from the trend exhibited by MD6K.

Figures 2 and 4 monitor parameters (I_E/I_M and $\tau_M/\langle\tau\rangle$) that probe the kinetics of excimer formation inside the polymer coil. They give credence to a blob approach to investigation of excimer formation along a polymer chain. According to Figures 2 and 4, a critical polymer chain length (cpcl) must be reached above which the process of excimer formation does not depend on polymer chain length, as predicted from a blob-based approach. As the polymer length decreases, it becomes comparable to the blob size, the cpcl is reached, and the kinetics of excimer formation do not obey the same scaling laws, as observed for MD6K. These measurements indicate that the cpcl for polystyrene in THF is between 6K and 40K.

To obtain a more detailed picture of the folding process taking place inside the polymer coil, we applied the blob model described in the Theory section to analyze the fluorescence decays. Equation 11 was used to fit the decays.

$$i_M(t) = f_1 \exp\{-(k_f + A_2)t - A_3[1 - \exp(-A_4 t)]\} + f_2 \exp(-k_f t) \quad (11)$$

In eq 11, k_f equals τ_M^{-1}, where τ_M is the natural lifetime of pyrene attached to the polystyrene chain. f_1 is the fraction of pyrene groups, which follow the blob model, and f_2 is the fraction of pyrene groups, which are located in pyrene-poor domains and cannot form excimer and fluoresce with the pyrene natural lifetime $\tau_M = k_f^{-1} =$ 257 ns. For the MD40K, MD110K and PD110K samples having a pyrene content between 1 and 9 mol %, f_2 was small and never larger than 0.18.

For the same pyrene content, f_2 was larger for MD6K. This reflects the increased partitioning of the pyrene groups with the shorter polymer. For instance, MD40K with a pyrene content λ equal to 10^{-4} mol/g has 4 pyrene groups per chain on average, whereas MD6K has only 0.6 pyrene group per chain for the same λ. The chance of having an isolated pyrene is much larger when dealing with MD6K leading to larger f_2 values.

Table 2. Parameters Retrieved from the Blob Model Analysis of the Pyrene Monomer Fluorescence Decays of Pyrene-Labeled MD6K in THF

sample M_n; M_w/M_n	pyrene (mol %)	λ ($\times 10^{-4}$ mol/g)	k_{diff} ($\times 10^7$ s^{-1})	$\langle n \rangle$	f_1	k_e[blob] ($\times 10^6$ s^{-1})	χ^2
MD6K	3.03	2.71	2.4	1.3	0.72	7.5	1.08
6000; 1.13	4.33	3.77	2.7	1.5	0.78	8.3	1.30
	8.86	7.02	2.4	2.3	0.91	5.4	1.14
	11.06	8.40	2.0	2.4	0.90	3.9	1.18

Table 3. χ^2 and f_1 Retrieved from the Blob Model Analysis of the Pyrene Monomer Fluorescence Decays of Pyrene-Labeled MD40K, MD110K, and PD110K in THF

sample M_n; M_w/M_n	pyrene (mol %)	λ ($\times 10^{-4}$ mol/g)	f_1	χ^2
MD110K	1.08	1.01	0.88	1.07
113 000; 1.03	1.26	1.17	0.82	1.06
	2.40	2.18	0.90	1.06
	2.54	2.30	0.98	1.25
	4.59	3.98	0.99	1.21
	7.03	5.78	0.98	1.28
MD40K	1.65	1.53	0.83	0.96
40 000; 1.04	2.23	2.20	0.93	1.18
	4.86	4.19	0.99	1.17
	5.98	5.03	0.98	1.03
PD110K	1.30	1.21	0.91	1.01
110 000; 1.48	3.17	2.83	0.93	1.27
	6.15	5.15	0.97	1.22
	6.29	5.25	0.99	1.03
	6.86	5.67	0.99	1.09

Equation 11 is equivalent to the equation commonly used for studying micellar systems by time-resolved fluorescence.[8,9,17] However, this is the first time that it is being applied to the study of polymer chains randomly labeled by pyrene. We also note that eq 11 uses five independent parameters, namely f_1, f_2, A_2, A_3, and A_4, the same number as that for eq 7. However, eq 7 provides a simple fit of the fluorescence decays with no physical meaning, whereas eq 11 provides a picture of how the excimer formation process occurs inside the polymer coil.

Equation 11 was then introduced into eq 9, and the resulting function $I_M(t)$ was compared with the experimental fluorescence decay. The parameters A_2, A_3, A_4, f_1, and f_2 were optimized using the Marquardt−Levenberg algorithm.[18] Equation 6 was used to obtain k_{diff}, $\langle n \rangle$, and k_e[blob] from the parameters A_2, A_3, and A_4. Because Figures 2 and 4 indicate that MD6K does not follow the same scaling law as do the longer polymers, the parameters retrieved from the fluorescence decays obtained with MD6K were listed in Table 2 but were not reported in Figures 5−9. f_1 and χ^2 for all polymers but MD6K are listed in Table 3. k_{diff}, $\langle n \rangle$ and k_e[blob] for polymers MD40K, MD110K, and PD110K are shown in Figures 6, 7, and 9, respectively. The errors in k_{diff}, $\langle n \rangle$, and k_e[blob] were estimated to be $\pm 0.1 \times 10^7$ s^{-1}, ± 0.2, and $\pm 0.7 \times 10^6$ s^{-1}, respectively. They were estimated by calculating the differences between the data points and the best fits given in Figures 6, 7, and 9.

Discussion

To prove the validity of the blob model, three *basic requirements* must be verified. First, eq 9, using eq 11 for $i_M(t)$, must fit the fluorescence decays well. Second, the parameters recovered from the blob model analysis, namely $\langle n \rangle$, k_{diff}, and k_e[blob] must have some reasonable, physical meaning. Third, polymer chain length should not affect the results.

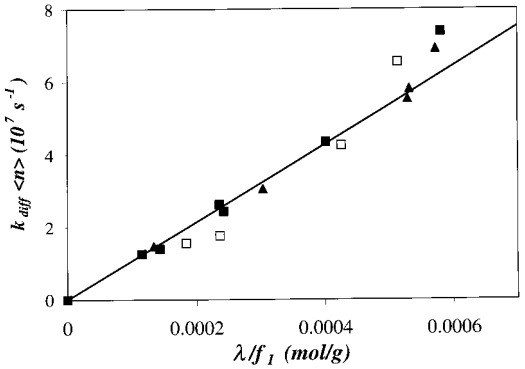

Figure 5. Plot of $k_{diff}\langle n \rangle$ versus λ/f_1 where the parameters k_{diff}, $\langle n \rangle$, and f_1 have been retrieved from the analysis of the monomer fluorescence decays (λ_{ex} = 344 nm, λ_{em} = 375 nm) with eq 11. □ MD40K, ■ MD110K, and ▲ PD110K.

The χ^2 listed in Tables 2 and 3 show that eq 9, using eq 11 for $i_M(t)$, does indeed fit the fluorescence decays well. All χ^2 values listed in Tables 2 and 3 are smaller than or equal to 1.3 (a perfect χ^2 equals 1.0). Furthermore, the residuals and the autocorrelation function of the residuals were randomly distributed around 0, again indicating that the fits were good. Thus, the first *basic requirement* for the validity of the blob model is fulfilled.

This also indicates that with the same number of parameters, the blob model expression (eq 11) better fits the fluorescence decays than the simple triexponential equation does (eq 8). However, whereas eq 8 only provides a fit of the decays with no physical meaning, eq 11 yields parameters that characterize the dynamics of the polymer chain considered.

Figure 5 represents the product $\langle n \rangle k_{diff}$ as a function of λ/f_1. By definition, k_{diff} is the rate constant of excimer formation inside a blob that contains one excited pyrene and one GS pyrene. k_{diff} depends on three variables: the viscosity of the solvent, the polymer chain flexibility, and the size of the blob. Because all experiments were carried out with the same polymer (polystyrene) and in the same solvent (THF), solvent viscosity and chain flexibility do not affect k_{diff}. Thus, k_{diff} depends only on the blob size in this study. k_{diff} is inversely proportional to the blob volume V_{blob}, according to eq 12.

$$k_{diff} \sim 1/V_{blob} \tag{12}$$

$\langle n \rangle$ is the average number of GS pyrene per blob. From eq 12 and the definition of $\langle n \rangle$, it results that, according to the predictions of the blob model, the product $\langle n \rangle k_{diff}$ is expected to be proportional to the local concentration of pyrene along the polymer backbone. The local concentration of pyrene is also proportional to λ/f_1, where λ is the average polymer content per gram of polymer and f_1 is obtained from eq 11. The correction $1/f_1$ is introduced to account for the volume fraction of polymer coil, which is not described by the blob model and where excited pyrenes do not form an excimer. In most cases, f_1 is very close to 1.0, and the factor $1/f_1$ accounts for a small correction. Figure 5 shows a linear relationship between $k_{diff}\langle n \rangle$ versus λ/f_1 up to pyrene contents of 8 mol %. This result indicates that the product $k_{diff}\langle n \rangle$ is a measure of the local concentration of pyrene groups along the polymer backbone, a parameter which is extremely useful but also extremely difficult to estimate by any other technique but the blob model approach.

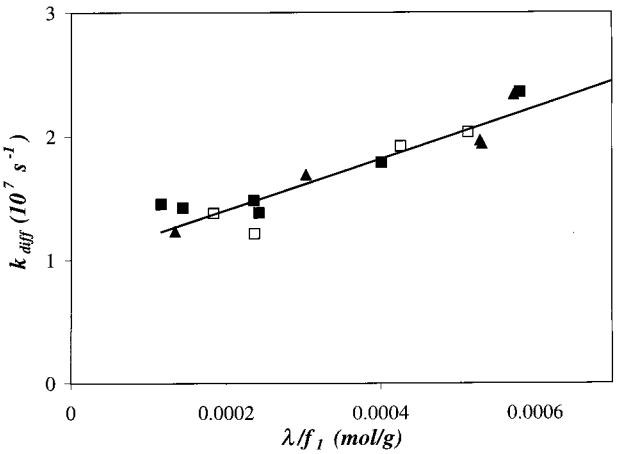

Figure 6. Plot of k_{diff} versus λ/f_1 where the parameters k_{diff} and f_1 have been retrieved from the analysis of the monomer fluorescence decays (λ_{ex} = 344 nm, λ_{em} = 375 nm) with eq 11. □ MD40K, ■ MD110K, and ▲ PD110K.

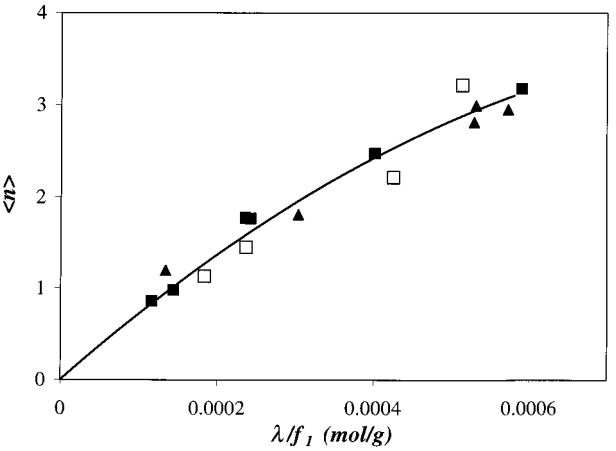

Figure 7. Plot of $\langle n \rangle$ versus λ/f_1 where the parameters $\langle n \rangle$ and f_1 have been retrieved from the analysis of the monomer fluorescence decays (λ_{ex} = 344 nm, λ_{em} = 375 nm) with eq 11. □ MD40K, ■ MD110K, and ▲ PD110K.

k_{diff} versus λ/f_1 is plotted in Figure 6. k_{diff} increases with pyrene content from 1.2×10^7 s^{-1} for a pyrene content of 1 mol % up to 2.2×10^7 s^{-1} for a pyrene content of 7 mol %. According to eq 12, this indicates that the blob volume V_{blob} or the blob size N_{blob} (expressed in styrene units per blob) decreases with increasing pyrene content. N_{blob} can be determined from the knowledge of $\langle n \rangle$, the average number of pyrene units per blob. $\langle n \rangle$ versus λ/f_1 is plotted in Figure 7. $\langle n \rangle$ increases quasilinearly with pyrene content. A linear fit is not perfect because the blob size does not remain constant with pyrene content and the data were fitted with a second-order polynomial. The size change of the blobs with pyrene content is confirmed in Figure 8, where the number of styrene units per blob (N_{blob}) is plotted as a function of λ/f_1. N_{blob} can be calculated from $\langle n \rangle$ and λ/f_1 according to eq 13:

$$N_{blob} = \frac{\langle n \rangle}{(\lambda/f_1)[354x + 104(1 - x)]} \qquad (13)$$

where x is the fraction of styrene units that are labeled, 354 represents the mass of a pyrene-labeled styrene unit and 104 represents the mass of an unlabeled styrene unit. As expected, N_{blob} decreases with pyrene content, which results in an increase in k_{diff}. N_{blob} reduces from

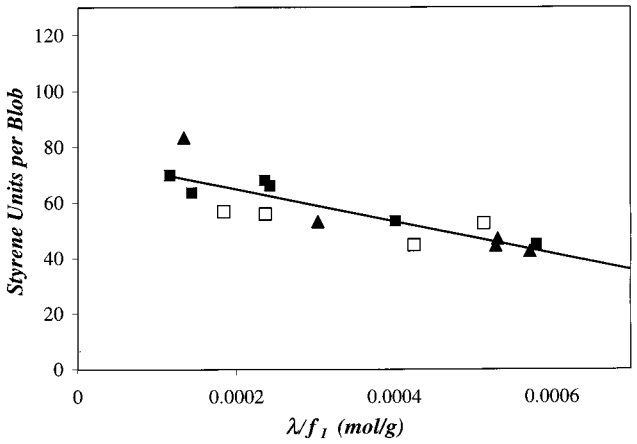

Figure 8. Plot of the number of styrene units per blob N_{blob} versus λ/f_1 where f_1 has been obtained from the analysis of the monomer fluorescence decays with eq 11 and N_{blob} has been obtained from eq 13. □ MD40K, ■ MD110K, and ▲ PD110K.

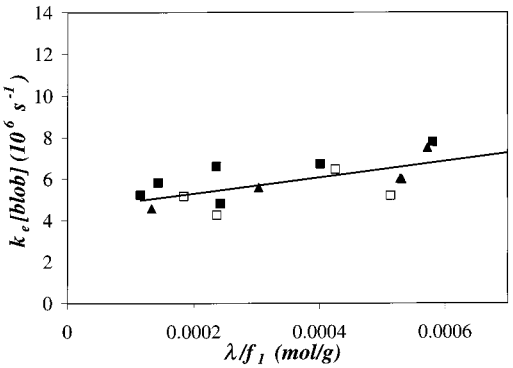

Figure 9. Plot of k_e[blob] versus λ/f_1 where the parameters k_e[blob] and f_1 have been retrieved from the analysis of the monomer fluorescence decays (λ_{ex} = 344 nm, λ_{em} = 375 nm) with eq 11. □ MD40K, ■ MD110K, and ▲ PD110K.

70 styrene units for a pyrene content of 1 mol % to 45 styrene units for a pyrene content of 7 mol %. It is remarkable that although both k_{diff} and $\langle n \rangle$ depend on pyrene content, the product $\langle n \rangle k_{diff}$ is proportional to the local pyrene concentration, as predicted by the blob model (cf. Figure 5). It is worthwhile to note that all N_{blob} values retrieved with polymers MD40K, MD110K, and PD110K are between 45 and 70 units/blob. MD6K is made of 57 styrene units. Its size is similar to that of a single blob, and it is understandable that the same scaling law, which applies to MD40K, MD110K, and PD110K, does not apply to MD6K.

The product k_e[blob] describes the exchange of GS pyrenes between blobs. k_e[blob] versus λ/f_1 is shown in Figure 9. Because N_{blob} decreases with pyrene content, [blob] must increase with pyrene content. Unfortunately, the parameter k_e[blob] retrieved from the analysis of the fluorescence decays yields scattered values. A linear fit of the data shows a linear increase of k_e[blob] with λ/f_1, but this relationship must be viewed with caution due to the scatter in the data.

At this stage, it is apparent that the trends observed (k_{diff} increases with λ/f_1 while N_{blob} decreases with λ/f_1; $k_{diff}\langle n \rangle$ increases linearly with λ/f_1) are internally consistent with the blob model theoretical framework.

It is worth noting that the values retrieved for the $\langle n \rangle$, k_{diff}, and k_e[blob] parameters are in the range of those obtained with an ethylene−propylene random copolymer labeled with pyrene studied in hexane.[7] This

system was much more complex because pyrene aggregates were present in the solution, and the polymer was polydisperse. However, a blob model analysis could handle the system satisfyingly, and the following values were obtained: $\langle n \rangle = 1.8 \pm 0.2$, $k_{diff} = 2.1 \pm 0.4 \times 10^7$ s^{-1}, and $k_e[blob] = 4.2 \pm 0.6 \times 10^6$ s^{-1}. These values appear to be very reasonable when compared to those obtained in this work. In this case, the product $k_{diff}\langle n \rangle$ represents the local concentration of pyrene aggregates within the polymer system.

This observation leads to the conclusion that the parameters, which are retrieved by using the blob model on polystyrene samples, are reasonable. Thus, the second *basic requirement* for establishing the validity of the model is verified.

The third *basic requirement* demands that the blob model yields parameters that are independent of chain length for chain lengths longer than the cpcl. This is a particularly interesting feature because it would permit the study of chain folding for inherently polydisperse polymeric systems. The trend shown in Figures 5−9 proves that this last requirement is observed. All parameters fall on single master curves regardless of their chain length as long as their chain length is longer than the cpcl.

$$k_{diff}\langle n \rangle \text{ (s^{-1} mol of pyrene/blob)} = 10.7 \times 10^9(\lambda/f_1) \text{ (mol/g)}$$

$$k_{diff} \text{ (s^{-1})} = 20.5 \times 10^9(\lambda/f_1) \text{ (mol/g)} + 10^7$$

$$\langle n \rangle \text{ (mol of pyrene/blob)} = -4.1 \times 10^6(\lambda/f_1)^2 \text{ (mol^2/g^2)} + 7700(\lambda/f_1) \text{ (mol/g)}$$

$$N_{blob} \text{ (styrene unit)} = -56 \times 10^3(\lambda/f_1) \text{ (mol/g)} + 75.5$$

$$k_e[blob] \text{ (s^{-1})} = 3.9 \times 10^9(\lambda/f_1) \text{ (mol/g)} + 4.5 \times 10^6 \text{ } s^{-1}$$

Many lines of evidence indicate that the blob model describes properly the polymeric systems investigated in this study. We can now use its framework to depict a more detailed picture of polymer dynamics inside a random coil. The blob model implies that for chain lengths longer than the cpcl chain folding is controlled by the local dynamics taking place within a blob. The folding rate constant within a blob is given by k_{diff}, which takes values between 1.2×10^7 and 2.2×10^7 s^{-1} (cf. Figure 6). For polystyrene samples, exchange between blobs occurs on a relatively slower time scale (k_e[blob] takes values between 4.9×10^6 and 6.8×10^6 s^{-1}). This indicates that for polystyrene chain folding occurs more efficiently within a blob and that exchange between blobs is less important. This follows from the fact that the distance being travelled by two chromophores both located inside the same blob is smaller than that between two chromophores located inside two different blobs. Understanding how the structure of the polymer affects the parameters k_{diff}, k_e[blob], and N_{blob} will contribute to better understanding of chain folding mechanisms.

Another implication of the blob model is that the chain dynamics depends on chain length when the chain length is shorter than the cpcl. Below the cpcl, the scaling law breaks down, and each chain has its own characteristic chain length-dependent folding mechanism. The existence of the cpcl has important implications for the study of the early folding stages (time < 10μs) of small proteins and peptides. Peptides having a chain length shorter than the cpcl should exhibit unique chain-folding mechanisms. Only when the chain length becomes longer than the cpcl can scaling laws be applied to investigate the folding pathways of large proteins.

This blob model can also be applied to more complicated polymers capable of forming associations.[7] The structures of proteins and RNA molecules or the associative strength of water-soluble associating polymers are the result of the subtle balance existing between the contents of hydrophobic and hydrophilic segments distributed along the polymer backbone. Because several hydrophobic units can combine into a single hydrophobic domain, determining the local concentration of hydrophobic domains is difficult because it is not proportional to the total number of hydrophobic residues. In this work, we have shown that, when no association is taking place between pyrene groups, the product $k_{diff}\langle n \rangle$ represents the local concentration of quenchers in the polymeric system and that it is proportional to the total number of pyrene groups (cf. Figure 5). If associations are taking place between pyrene groups, the product $k_{diff}\langle n \rangle$ still represents the local concentration of quenchers in the polymeric system. However, the quenchers are the pyrene aggregates within the polymeric network, and the product $k_{diff}\langle n \rangle$ now characterizes the local concentration of hydrophobic aggregates within the polymeric network. The product $k_{diff}\langle n \rangle$ can help to characterize the associative strength of a biological or synthetic polymer chain, with a more associating chain taking a larger $k_{diff}\langle n \rangle$ value.

Because pyrene is a bulky molecule, the changes in k_{diff} and N_{blob} with pyrene content that we have observed in this study could be a consequence of having introduced the pyrene label into the polymeric system. However, it is possible to estimate how this system would behave ideally were no pyrene present, by extrapolating the trends shown in Figures 5−9 to a pyrene content of 0.0 mol %. According to this procedure, an ideal blob would be made of 75 styrene units with an associated excimer formation rate constant k_{diff} of 1.0×10^7 s^{-1} and an exchange rate k_e[blob] of 4.5×10^6 s^{-1}. Interestingly this ideal blob size is similar to the size of a polymer chain for which a segment located at its center is no longer affected by the faster dynamics of the chain ends.[20] Further studies will establish how the parameters $\langle n \rangle$, k_{diff}, and k_e[blob] vary with the nature of the solvent and the monomer structure, and they will lead to a better understanding of the folding mechanisms of synthetic and biological polymers.

Conclusion

Fluorescence spectroscopy was used to monitor the dynamics of chain folding. The chain studied was polystyrene. The pyrene chromophore was covalently attached onto the polymer backbone, and the process of excimer formation was monitored by steady-state and time-resolved fluorescence spectroscopy. The complicated kinetics of excimer formation was handled quantitatively by introducing the concept of blob into the analysis. Within the framework of this analysis, the polymer dynamics can be handled with only three parameters, namely, $\langle n \rangle$, k_{diff}, and k_e[blob]. Four major conclusions were established in this work. First, the blob

model analysis properly describes the fluorescence decays of polymers that have been randomly labeled with the chromophore pyrene and when the pyrene monomer fluorescence is quenched by excimer formation. Second, the blob model does not depend on polymer polydispersity, as it is expected with any blob-based analysis. Third, the blob model yields information about the local concentration of pyrene groups within the polymer coil. This aspect of the blob model will be very helpful to the characterization of polymers whose properties have been modified by random grafting of the chain with specific pendants, a practice frequently encountered in polymer science. Fourth, scaling laws can be applied to monitor chain folding as long as the chain length is longer than the cpcl. For chain lengths shorter than the cpcl, each chain will have a specific chain-folding mechanism. It is our expectation that further analyses based on the blob model will help us deepen our understanding of chain folding of synthetic and biological polymers.

Acknowledgment. We thank NSERC for financial support and Dr. Manhar Lad, Dr. Mario Gauthier, and Andy Kee (University of Waterloo) for their help with the synthesis and labeling of the polystyrene samples.

References and Notes

(1) Guillet, J. E. *Polymer Photophysics and Photochemistry*; Cambridge University Press, New York, 1985. Lakowicz, J. R. *Principles of Fluorescence Spectroscopy*; Plenum Press, New York, 1986. Morawetz, H. *J. Lumin.* **1989**, *43*, 59−71. Webber, S. E.; Munk, P.; Tuzar, Z. *Solvents and Self-Organization of Polymers;* NATO ASI Series, Series E: Applied Science; 1996; Vol 327. Allen, S. N. *Photochemistry*; Gilbert, A., Ed.; The Royal Society of Chemistry, 1996.
(2) Winnik, M. A. *Acc. Chem. Res.* **1985**, *18*, 73−79.
(3) Birks, J. B. *Photophysics of Aromatic Molecules*; Wiley: New York, 1970; p 301.
(4) Winnik, M. A.; Li, X.-B.; Guillet, J. E. *Macromolecules* **1984**, *17*, 699−702.
(5) Winnik, M. A.; Egan, L. S.; Tencer, M.; Croucher, M. D. *Polymer* **1987**, *28*, 1553−1560.
(6) Duhamel, J.; Yekta, A.; Winnik, M. A.; Jao, T.-C.; Mishra, M. K.; Rubin, I. D. *J. Phys. Chem.* **1993**, *97*, 13708−13712.
(7) Vangani, V.; Duhamel, J.; Nemeth, S.; Jao, T.-C. *Macromolecules* **1999**, *32*, 2845−2854.
(8) Dederen, J. C.; van der Auweraer, M.; De Schryver, F. C. *J. Phys. Chem.* **1981**, *85*, 1198−1202.
(9) (a) Tachiya, M. *Chem. Phys. Lett.* **1975**, *33*, 289−292. (b) Infelta, P. P.; Gratzel, M.; Thomas J. K. *J. Phys. Chem.* **1974**, *78*, 190−195.
(10) (a) Yekta, A.; Xu, B.; Duhamel, J.; Adiwidjaja, H.; Winnik, M. A. *Macromolecules* **1995, *28,*** 956−966. (b) Alami, E.; Almgren, M.; Brown, W. *Macromolecules* **1996**, *29*, 5026−5035.
(11) de Gennes, P.-G. *Scaling Concepts in Polymer Physics*; Cornell University Press: Ithaca, NY, 1979.
(12) Gauthier, M.; Möller, M. *Macromolecules* **1991**, *24*, 4548−4553. Swarc, M.; Levy, M.; Milkovich, R. *J. Am. Chem. Soc.* **1956**, *78*, 2656−2657.
(13) Frank, R. S.; Merkle, G.; Gauthier, M. *Macromolecules* **1997**, *30*, 5397−5402.
(14) Chong, J. M.; Shen, L. *Synth. Commun.* **1998**, *28*, 2801−2806.
(15) Demas, J. N. *Excited-State Lifetime Measurements*; Academic Press, New York, 1983; p 102.
(16) (a) Berlman, I. B. *Handbook of Fluorescence Spectra of Aromatic Molecules*; Academic Press: New York, 1971. (b) Measured on Pr. M. A. Winnik (U. of Toronto, Canada) picosecond time-resolved fluorometer.
(17) Yekta, A.; Aikawa, M.; Turro, N. J. *Chem. Phys. Lett.* **1979**, *63*, 543−548.
(18) Press, W. H.; Flannery, B. P.; Teukolsky, S. A.; Vetterling, W. T. *Numerical Recipes. The Art of Scientific Computing (Fortran Version)*; Cambridge University Press: Cambridge, 1992.
(19) Lee, S.; Duhamel, J. *Macromolecules* **1998**, *31*, 9193−9200. Chu, D. Y.; Thomas, J. K. *Macromolecules* **1984**, *17*, 2142−2147.
(20) Horinaka, J.-I.; Maruta, M.; Ito, S.; Yamamoto, M. *Macromolecules* **1999**, *32*, 1134−1139.
(21) Chuprina, V. P.; Rullmann, J. A. C.; Lamerichs, R. M. J. N.; van Boom, J. H.; Boelens, R.; Kaptein, R. *J. Mol. Biol.* **1993**, *234*, 446−462.

MA990702C